Fluorescence biosensor for ultrasensitive detection of the available lead based on target biorecognition-induced DNA cyclic assembly

Junhua Chen [a,b], Manjia Chen [b], Hui Tong [b], Fei Wu [a], Yizhang Liu [a], Chengshuai Liu [a,*]

[a] State Key Laboratory of Environmental Geochemistry, Institute of Geochemistry, Chinese Academy of Sciences, Guiyang 550081, China
[b] National-Regional Joint Engineering Research Center for Soil Pollution Control and Remediation in South China, Guangdong Key Laboratory of Integrated Agro-environmental Pollution Control and Management, Institute of Eco-environmental and Soil Sciences, Guangdong Academy of Sciences, Guangzhou 510650, China

HIGHLIGHTS

- DNAzyme biorecognition-induced DNA cyclic assembly was used to construct the biosensor.
- Hairpin probes were used to build the Y-shaped sensing scaffold.
- The linear range of the biosensor is from 1 pM to 100 nM and the detection limit is 0.2 pM.
- The assay is robust and has been applied to the detection of the available lead in soil samples.

GRAPHICAL ABSTRACT
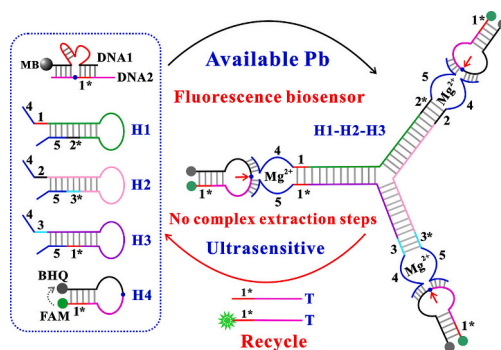
ARTICLE INFO

ABSTRACT

A fluorescence biosensor was developed for the ultrasensitive detection of the available lead in soil samples by coupling with DNAzyme and hairpin DNA cyclic assembly. The biorecognition between lead and 8-17 DNAzyme will cleave the substrate strands (DNA2) and release the trigger DNA (T), which can be used to initiate the DNA assembly reactions among the hairpins (H1, H2, and H3). The formed Y-shaped sensing scaffold (H1-H2-H3) contains active Mg^{2+}-DNAyzmes at three directions. In the presence of Mg^{2+}, the BHQ and FAM modified H4 will be cleaved by the Mg^{2+}-DNAyzme to generate a high fluorescence signal for lead monitoring. The linear range of the fluorescence biosensor is from 1 pM to 100 nM and the detection limit is 0.2 pM. The biosensor also exhibited high selectivity and the nontarget competing heavy metals did not interfere with the detection results. Compare with the traditional method (DTPA+ICP-MS) for the available lead detection, the relative error (Re) is in the range from -8.3 % to 9.5 %. The results indicated that our constructed fluorescence biosensor is robust, accurate, and reliable, and can be applied directly to the detection of the available lead in soil samples without complex extraction steps.

* Corresponding author.
  E-mail address: liuchengshuai@vip.gyig.ac.cn (C. Liu).

1. Introduction

Heavy metal accumulation in soil samples is a major issue of global concern because the transfer of heavy metals from soil samples into crops will affect food safety and human health (Malematja et al., 2023). The heavy metal-mediated toxicity on ecosystem and human health usually depends on the available metal concentrations rather than the total amount in the environment (Ibrahim et al., 2022). The free ions of heavy metals in soil samples are generally considered as the key species that control their availability for plants (Gao et al., 2022; Parker and Pedler, 1997). One can define the available metal as the soluble, ionic, and the easily released form of the metal, which can interact with surrounding plant cells or other biota (Rensing and Maier, 2003). As one of the widely distributed heavy metals, the available lead can cause neurological, cardiovascular, and nephritic disorders even at low concentrations due to its bioaccumulative and nonbiodegradable nature (Liang et al., 2023; Yang et al., 2023). Considering the detrimental effects of the available lead, developing simple, sensitive, and selective methods for the available lead detection is of great significance.

Traditional methods for the available lead detection focused on atomic absorption spectrometry (AAS), atomic fluorescence spectrometry (AFS), inductively coupled plasma optical emission spectrometer (ICP-OES), and inductively coupled plasma mass spectrometer (ICP-MS) (Mao et al., 2021; Xu et al., 2022). Although these methos are sensitive and accurate, they usually require complicated sample extraction procedures, such as DTPA method (Lindsay and Norvell, 1978), BCR extraction (Ure et al., 1993), and Tessier protocol (Tessier et al., 1979). Thus, it is highly desirable to develop a rapid, convenient, and reliable method for the detection of the available lead without complex extraction steps. Some interesting electrochemical sensors based on nanocomposite platforms have been reported for lead detection and they exhibited good selectivity (Deshmukh et al., 2018a, 2018b, 2018c). To date, fluorescence biosensor has also attracted considerable attention due to the advantages of easy modification, rapid response, simple operation, and cost-effective and convenient preprocessing (Geng et al., 2020; Yang et al., 2022a). In order to detect the trace concentrations of available heavy metal in complex soil samples, the detection sensitivity of fluorescence biosensor should be further improved.

One way to improve the sensitivity is through signal amplification (Lan et al., 2019; Xu et al., 2018, 2019). Some elegant signal amplification strategies have been reported for lead detection (Huang et al., 2019; Liu et al., 2019; Meng et al., 2020; Miao et al., 2011; Wen et al., 2017; Yao et al., 2019), such as using nanomaterials as the labels or using protein enzyme as the tools (Ji et al., 2019; Li et al., 2022; Rajaji and Panneerselvam, 2020; Yang et al., 2022b). The synthesis of nanomaterials is a complex process and the leakage of the nanomaterial may even pollute the environment (El-Kady et al., 2023). The protein enzyme is susceptible to temperature and environmental parameter, which may affect the analytical performance in complex samples (Li et al., 2023). As an alternative, the nanomaterial-free and protein enzyme-free biosensor based on pure DNA assembly has the advantage of high stability, environment friendly, and efficient signal amplification (Guan et al., 2021; Lv et al., 2022; Suo et al., 2023; Teng et al., 2023; Wang et al., 2022a, 2022b; Zhao et al., 2022). In this work, we developed a fluorescence biosensor for the available lead detection based on DNA cyclic assembly. Using Pb^{2+} as a standard species of the available lead, the 8–17 DNAzyme (Brown et al., 2003; Liu and Lu, 2004; McConnell et al., 2021; Zheng et al., 2021) was used as the molecular recognition element to recognize the available lead in soil samples. The available lead can recognize the probe of the 8–17 DNAzyme to cleave the substrate chain of the probe. The released substrate chain then can be used to trigger the DNA cyclic assembly. Through continuous assembly reactions among the hairpin probes (H1, H2, and H3), the formed H-H2-H3 products containing Mg^{2+}-DNAzymes in the Y-shaped sensing scaffold can cleave the BHQ-FAM labelled H4 to give a high fluorescence signal for output.

2. Experimental section

2.1. Chemicals and materials

DNA probes were ordered from Shanghai Sangon Biotechnology Co., Ltd. (Shanghai, China) and the sequences were listed in Table S1 (Supporting Information). Streptavidin (SA)-coated magnetic beads (MB, 1 μM in diameter) were purchased from Shanghai Aladdin Biochemical Technology Co., Ltd. (Shanghai, China). Other chemicals were purchased from Sigma-Aldrich (Merck KGaA, Darmstadt, Germany). Milli-Q water (18.2 MΩ/cm) was used in the experiments.

2.2. Procedure for lead detection

All DNA probes were separately heated at 95 °C for 10 min and then gradually cooled down to room temperature at a constant rate of 1 °C/min. 100 nM biotinylated DNA1 and 130 nM DNA2 were added to the SA-coated MB solution (200 μL, 1.2 mg/mL) and incubated at room temperature for 30 min with gentle shaking. After magnetic separation and washing three times with the washing buffer (20 mM PBS, 0.01 % Tween-20, pH 7.4), the resulting MB-DNA1-DNA2 conjugates were redispersed in the reaction buffer (20 mM Tris-AC, 100 mM NaAC, 50 mM MgAC$_2$, pH 7.4). Different concentrations of lead were added to the MB-DNA1-DNA2 conjugates and incubated at room temperature for 40 min. After magnetic separation, the supernatant was transferred to 250 nM H1, 250 nM H2, 250 nM H3, and 400 nM H4 and incubated at room temperature for 60 min. The fluorescence spectra of the solution were recorded by the SpectraMax i3x (Molecular Devices, San Jose, USA).

2.3. Procedure of real sample analysis

The soil samples were collected from an agricultural field near South China Botanical Garden (Guangzhou, China). After air-drying, the soil was sieved to pass through 0.15 mm mesh and homogenized thoroughly. We used two methods to detect the available lead in soil samples: DTPA method and fluorescence biosensor. For the DTPA method, the DTPA extracting solution was prepared to contain 10 mM CaCl$_2$, 100 mM triethanolamine, and 5 mM DTPA in deionized water matrix. The pH of the extracting solution was adjusted to 7.3 by addition of HCl. 10 g soil and 20 mL DTPA extracting solution were mixed and shaken on a horizontal shaker at 160 cycles/min for 2 h. After centrifugation at 5000 rpm for 10 min, the supernatant was filtered through Whatman No. 42 filter paper. The filtrates were used to analyze the available lead using inductively coupled plasma mass spectrometer (ICP-MS). For the fluorescence biosensor assay, the homogenized soil samples were directly added to the reaction buffer containing DNA1-DNA2 and incubated at room temperature (about 25 °C) for 40 min. After magnetic separation, the supernatant was transferred to the reaction buffer containing H1, H2, H3 (250 nM) and H4 (400) nM. Other procedures were the same as described in the section of "Procedure for lead detection".

2.4. Native polyacrylamide gel electrophoresis (PAGE)

The details of the native PAGE procedures were listed in the Supporting Information.

3. Results and discussion

3.1. Sensing principle

The sensing principle of the fluorescence biosensor for the available lead detection is illustrated in Scheme 1. The 8–17 DNAzyme was used to recognize the available lead. MB-modified DNA1 is the DNAzyme strand of 8–17 DNAzyme and DNA2 is the substrate strand containing a ribonucleoside adenosine (rA, indicated in blue). In the presence of the available lead, DNA2 was cleaved into two fragments at the rA position
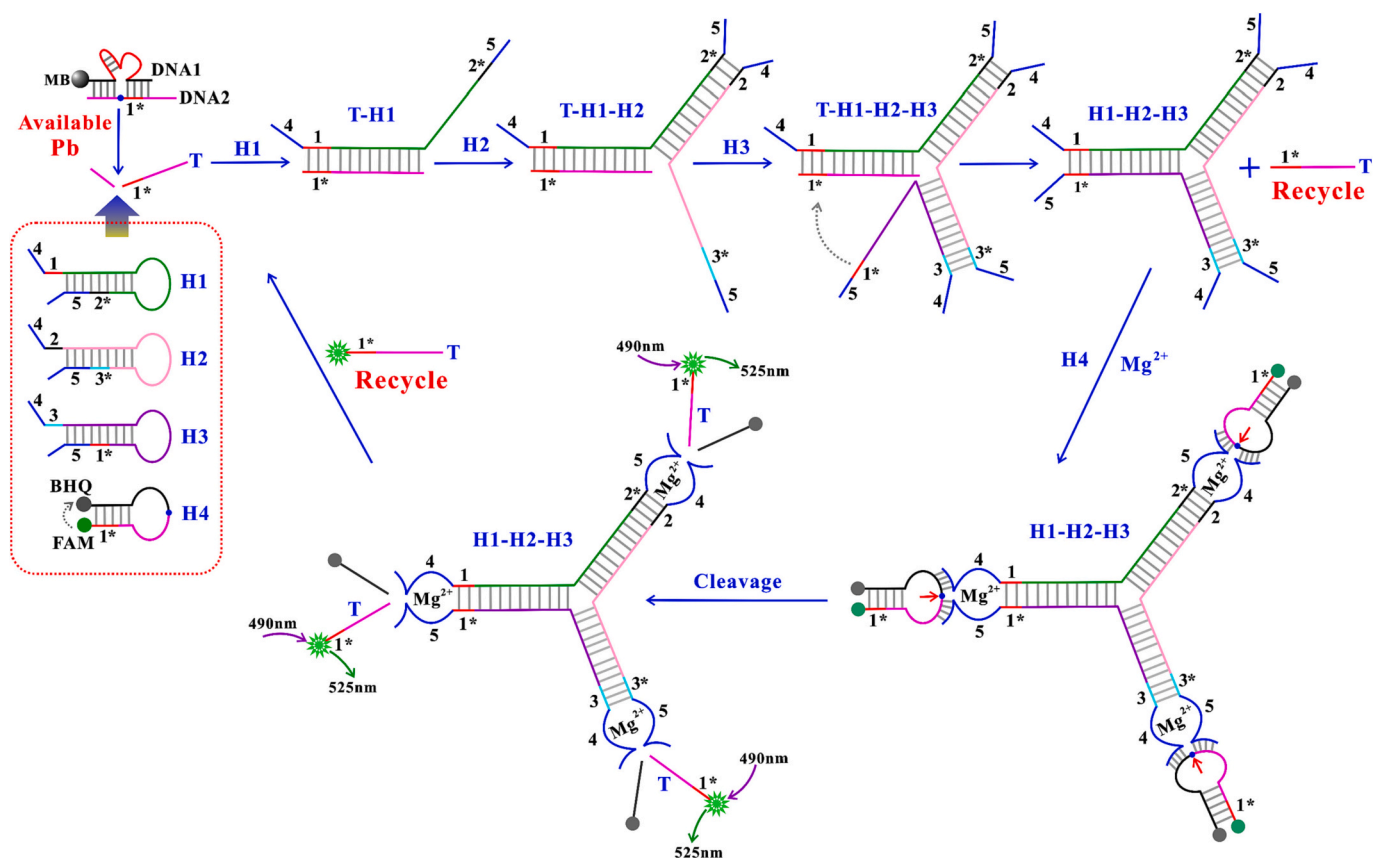
Scheme 1. The sensing principle of the fluorescence biosensor for the available lead detection based on heavy metal biorecognition-induced DNA cyclic assembly. DNA1 and DNA2 are the biorecognition elements, in which DNA1 is immobilized on magnetic beads (MB). The hairpin probes H1, H2, and H3 are used to construct the Y-shaped sensing scaffold. The hairpin probe H4 modified with FAM and BHQ is used as the signal reporter.

due to the specific biorecognition between the available lead and DNAzyme. After magnetic separation, the trigger strand (T) was used to activate the cyclic assembly reactions among H1, H2, and H3. The exposed domain 1* of T serves as a toehold to bind with the domain 1 of H1 and initiates toehold-mediated strand displacement to open H1, resulting in the formation of the T-H1 intermediate where the domain 2* of H1 is opened. The newly opened toehold 2* of H1 can further hybridize to the domain 2 of H2, again initiating toehold-mediated strand displacement to open H2 and form the T-H1-H2 complex where the domain 3* of H2 is also opened. Similarly, the domain 3 of H3 can interact with the domain 3* of H2 to open H3 and generate the T-H1-H2-H3 hybrid. T will spontaneously depart from the hybrid and form the stable H1-H2-H3 product. The released T can be recycled to activate the assembly reactions of additional hairpins that can produce numerous H1-H2-H3 products. The DNA hairpins of H1, H2, and H3 contain the split sequences of the Mg^{2+}-DNAyzme at their two termini (domains 4 and 5). The successfully assembled H1-H2-H3 product can bring the split sequences into close proximity to form active Mg^{2+}-DNAyzmes at three directions in the Y-shaped sensing scaffold. In the presence of Mg^{2+}, the substrate strand (H4) will be cleaved by the Mg^{2+}-DNAyzme. The separation of FAM and BHQ will generate a high fluorescence signal. Importantly, the released DNA fragment has the same sequence as the trigger DNA (T), which can also be recycled to activate the assembly reactions of H1, H2, and H3. Through the DNA cyclic assembly processes, the fluorescence biosensor can realize the ultrasensitive detection of the available lead.

3.2. Feasibility verification

To evaluate the feasibility of the biosensor for the available lead

detection, the fluorescence signals were recorded under different conditions. As shown in Fig. 1A, the mixture of DNA1-DNA2, H1, H2, H3, and H4 without Pb^{2+} only yielded a background signal (curve a). The solution of DNA1-DNA2, Pb^{2+}, H1, and H4 also generated a weak response compared with curve a (curve b), indicating that the formed T-H1 complex failed to generate an active Mg^{2+}-DNAzyme. In the presence of DNA1-DNA2, Pb^{2+}, H1, H2, and H4, a slight fluorescence recovery can be observed (curve c) because of the formation of an active Mg^{2+}-DNAzyme at one end of the T-H1-H2 complex, which can cleave H4 to give a fluorescence signal. When all the sensing elements (DNA1-DNA2, Pb^{2+}, H1, H2, H3, and H4) existed in the solution, the fluorescence signal improved sharply (curve d), implying the successful assembly of the H1-H2-H3 products and the recycled T can improve the detection sensitivity. The corresponding fluorescence intensity at 525 nm was recorded in the Inset of Fig. 1A. The hybridization of DNA was further verified by circular dichroism (CD) spectroscopy and the results were shown in Fig. S1 (Supporting Information).

The native polyacrylamide gel electrophoresis (PAGE) was further carried out to confirm the feasibility of the hairpin assembly. As shown in Fig. 1B, the band in lane 1 corresponded to H1. Mixing T with H1 can generate a band of T-H1 complex in lane 2. H2 then can react with T-H1 to produce a band that corresponded to the complex T-H1-H2 (lane 3). The band in lane 4 with low mobility should be mainly composed of the H1-H2-H3 product, which was formed through the step-wise reaction of T, H1, H2, and H3. Those results successfully verified the feasibility of the fluorescence biosensor for the available lead detection based on DNA cyclic assembly.
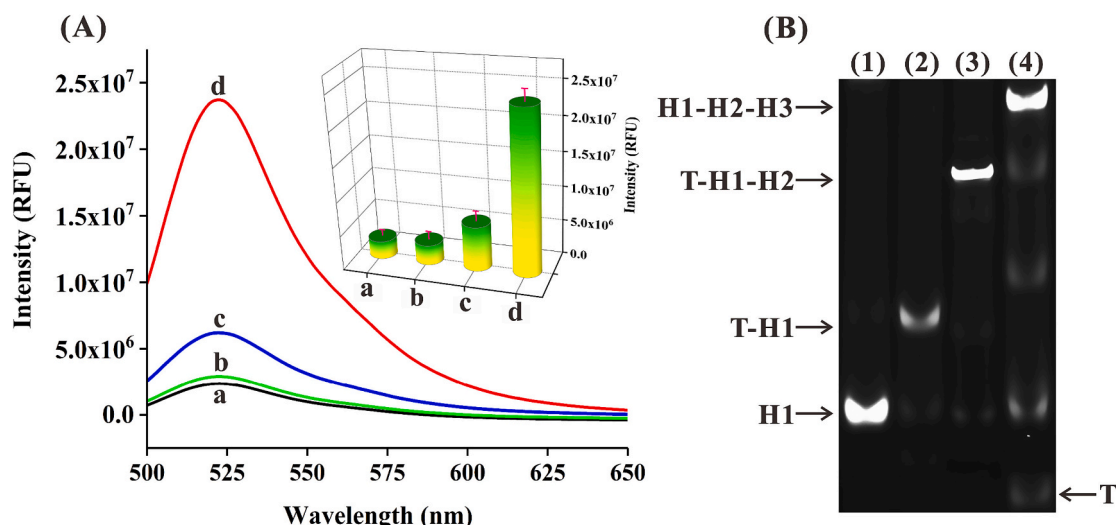
Fig. 1. (A) Fluorescence responses of the sensing system under different conditions. (a): DNA1-DNA2 + H1 + H2 + H3 + H4. (b): DNA1-DNA2 + Pb^{2+}+H1 + H4. (c): DNA1-DNA2 + Pb^{2+}+H1 + H2 + H4. (d): DNA1-DNA2 + Pb^{2+}+H1 + H2 + H3 + H4. Inset: The corresponding fluorescence intensity of the solution at 525 nm. (B) Native PAGE verification of the hairpin assembly among H1, H2, and H3. Lane 1: H1. Lane 2: T + H1. Lane 3: T + H1 + H2. Lane 4: T + H1 + H2 + H3. Concentrations for each DNA in PAGE are 1 μM.

3.3. Analytical performance

To obtain the best analytical performance of the fluorescence biosensor for the available lead detection, some experimental conditions, such as the hairpin concentration (H1, H2, and H3), the assembly time among the hairpins, the reaction temperature, and the pH of the buffer solution were optimized. As shown in Fig. 2A, with the increase of the hairpin concentration (H1, H2, and H3) from 50 to 350 nM, the fluorescence intensity increased in the presence of 10 nM Pb^{2+}. At the same time, the background signal kept increasing with the concentration increased. The signal-to-noise ratio (S/N) reached a maximum when the concentration reached 250 nM. Thus, the optimal hairpin concentration (H1, H2, and H3) is 250 nM. The effect of the assembly time among the hairpins was also optimized. As shown in Fig. 2B, the fluorescence signal increased with the augment of the assembly time from 10 to 60 min and reached a plateau after 60 min. The results indicated that the assembly reaction the hairpins can be completed in 60 min. Thus, we choose 60 min as the optimal assembly time. The effects of the reaction temperature and the pH of the buffer solution on the fluorescence responses of the biosensor were further optimized and the results were shown in

Figs. S2 and S3 (Supporting Information).

Under the optimal experimental conditions, the fluorescence biosensor was used to detect Pb^{2+} with different concentrations. As the Pb^{2+} concentrations increased from 0 to 500 nM, the corresponding fluorescence signals increased gradually and the fluorescence spectra of the biosensor were recorded in Fig. 3A. The FAM fluorescence intensities at 525 nm were recorded in Fig. 3B. The resulting calibration curve shows that the fluorescence intensity is proportional to the logarithm of Pb^{2+} concentration in the range of 1 pM-100 nM (Fig. 3B, inset). The linear regression equation is: $F = 4.58 \times 10^6 + 4.67 \times 10^6$ Lg C ($R^2 = 0.996$), where F is the fluorescence intensity and C is the Pb^{2+} concentration. The limit of detection (LOD) is calculated to be 0.2 pM based on 3S/N rule. Compared with the protein enzyme and nanomaterial-based lead sensors (Chen et al., 2020; Song et al., 2019), our constructed nanomaterial-free and protein enzyme-free biosensor exhibited a higher sensitivity. Compared with some previously reported Pb^{2+} detectors, our proposed fluorescence biosensor also has comparable or more sensitive detection limit (Table S2, Supporting Information). The high sensitivity can be primarily attributed to the continuous DNA assembly reactions in the dual signal amplification pathways, which can generate
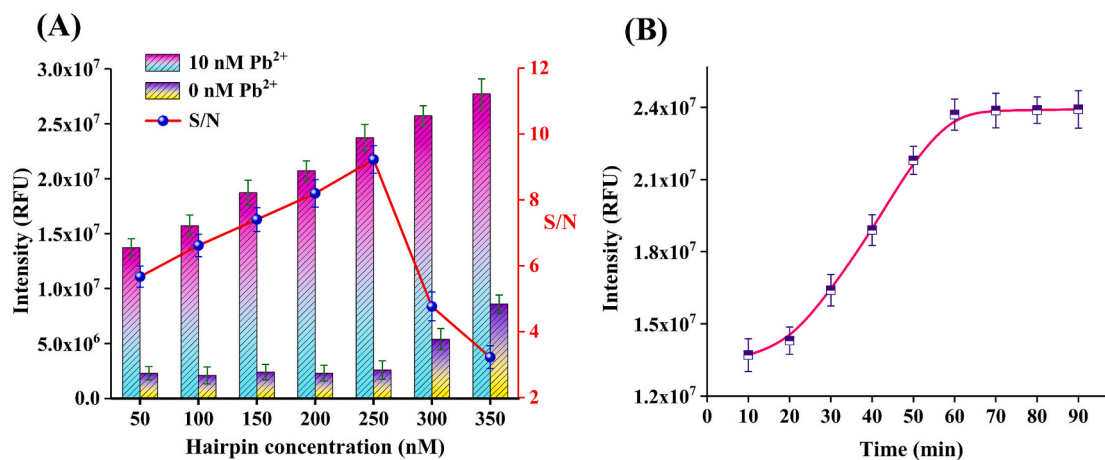

Fig. 2. (A) Effect of hairpin concentration (H1, H2, and H3) on the fluorescence response of the biosensor. DNA1: 100 nM; DNA2: 130 nM; H4: 400 nM. The experiments were performed at room temperature. (B) Effect of the assembly time among the hairpins on the fluorescence response of the biosensor. DNA1: 100 nM; DNA2: 130 nM; H1, H2, and H3: 250 nM; H4: 400 nM. Pb^{2+}: 10 nM. The experiments were performed at room temperature.
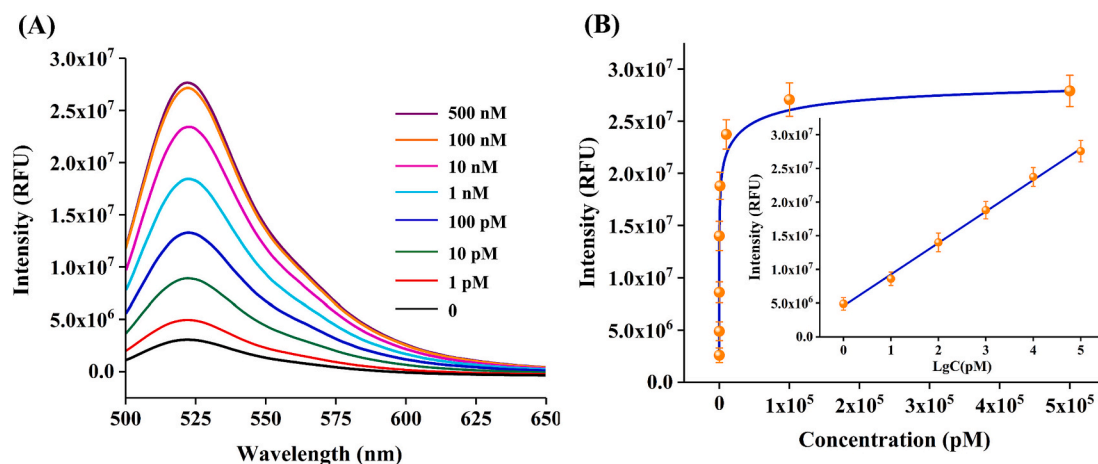
Fig. 3. (A) Fluorescence spectra of the biosensor upon the addition of different concentrations of Pb^{2+}. (B) Plots of the fluorescence intensity at 525 nm as a function of the Pb^{2+} concentration. Inset: Linear relationship between the fluorescence intensity and the logarithm of Pb^{2+} concentration in the range from 1 pM to 100 nM.

numerous H1-H2-H3 products even at low concentration of the available lead.

3.4. Selectivity of the biosensor

To investigate the selectivity of the fluorescence biosensor, the control interfering ions, including Hg^{2+}, Cu^{2+}, Cr^{3+}, Fe^{2+}, Mn^{2+}, Sn^{2+}, Al^{3+}, Ag^+, and their mixture were examined in the same condition as that for Pb^{2+} detection. As shown in Fig. 4, the fluorescence signals of the biosensor towards the control heavy metal ions and the mixture are almost as the same as the blank samples. In the presence of Pb^{2+}, the fluorescence signals enhanced dramatically. In addition, when adding Pb^{2+} to the control interferent mixture, the biosensor also exhibited a high fluorescence response. Such excellent selectivity of the fluorescence biosensor can be ascribed to the specific biorecognition between Pb and the 8–17 DNAzyme.

3.5. Real sample analysis

To validate the practicability and reliability of the fluorescence biosensor, the sensing system was used to detect the available Pb in soil samples. For the conventional detection method, the available Pb in soil samples were extracted by the DTPA method and then quantified by the ICP-MS method. For the fluorescence biosensor method, the homogenized soil samples were directly added to the reaction buffer for assay without complex extraction steps. As shown in Table 1, the biosensor detection results have good consistency with the ICP-MS method. The relative standard deviation (RSD) of the fluorescence biosensor was below 5 %. The relative error (Re) between the DTPA + ICP-MS and the fluorescence biosensor was from −8.3 % to 9.5 %. These results indicated that our proposed fluorescence biosensor is robust and can be used to directly detect the available Pb without complex extraction steps in soil samples with good accuracy and reliability.

4. Conclusions

In conclusion, we have successfully constructed a fluorescence biosensor for the ultrasensitive detection of the available lead on the basis of DNAzyme biorecognition and hairpin DNA probes assembly. In the presence of the available lead, the released trigger strand (T) can activate the hairpin assembly among H1, H2, and H3 to produce the Y-shaped sensing scaffold (H1-H2-H3) through toehold-mediated strand displacement reactions. In the H1-H2-H3 products, the formed active Mg^{2+}-DNAyzmes at the three arms can cleave H4 to produce the fluorescence signal for the available lead detection. Importantly, the strand T can be recycled to trigger the continuous assembly reactions among the hairpins, which can realize the signal amplification purpose. Our constructed sensing system has three characteristics: (1) The dual signal amplification pathways in the platform can effectively improve the detection sensitivity. The detection limit of the fluorescence biosensor is 0.2 pM, which exhibits a higher sensitivity compared with some
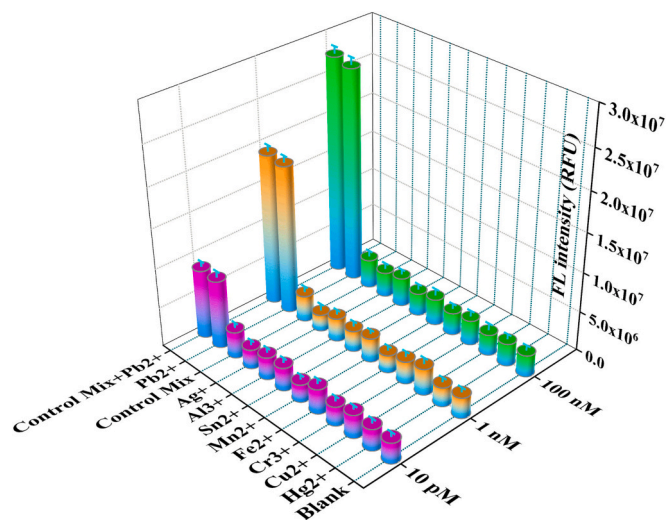
Table 1
Detection of the available Pb in soil samples using the fluorescence biosensor and the conventional DTPA + ICP-MS method.

Samples	ICP-MS[a]	Biosensor[b]	RSD[c] (%)	Re[d] (%)
Soil 1#	0.26 nM	0.24 nM	3.7	−8.3
Soil 2#	7.45 nM	7.98 nM	4.5	6.6
Soil 3#	15.36 nM	16.97 nM	4.2	9.5
Soil 4#	28.78 nM	27.16 nM	3.8	−5.9
Soil 5#	75.92 nM	79.84 nM	4.9	4.9

[a] The available Pb was extracted by DTPA method and detected by inductively coupled plasma mass spectrometer (ICP-MS).
[b] Fluorescence biosensor detection using 8–17 DNAzyme as the biorecognition element ($n = 3$).
[c] Relative standard deviation (n = 3).
[d] Relative error: Proposed fluorescence biosensor vs. ICP-MS.

Fig. 4. Selectivity results of the fluorescence biosensor for Pb^{2+} and several competing heavy metal ions. 10 pM, 1 nM, and 100 nM Pb^{2+} and control ions were tested in the same condition.

previously reported lead detectors. (2) The assay method eliminates protein enzyme and nanomaterial label, which facilitates the simple, rapid, and environment friendly detection of the available lead in complex samples. The biosensor is robust and can be used to detect Pb in real soil samples with good accuracy and reliability. The relative standard deviation (RSD) of the fluorescence biosensor was below 5 %. (3) Compared with the traditional sequential extraction procedure, the fluorescence biosensor can realize the fast detection of the available lead without complex extraction steps. This is an end-user friendly sensor and the operation is simple. We have applied the sensing system to the detection of the available lead in soil sample with good accuracy and reliability compared with the traditional DTPA + ICP-MS method. We think our proposed sensing platform can serve as a useful tool for the ultrasensitive and reliable detection of other available heavy metals by simply choosing other heavy metal-specific nucleic acids as molecular recognition elements.

Declaration of competing interest

None.

Data availability

Data will be made available on request.

CRediT authorship contribution statement

Junhua Chen: Conceptualization, Methodology, Data curation, Writing-original draft, review & editing. **Manjia Chen:** Methodology, Validation, Resources. **Hui Tong:** Methodology, Data curation, Validation. **Fei Wu:** Methodology, Formal analysis. **Yizhang Liu:** Formal analysis, Resources. **Chengshuai Liu:** Funding acquisition, Project administration, Writing-review & editing.

Appendix A. Supplementary data

Supplementary data to this article can be found online at https://doi.org/10.1016/j.scitotenv.2023.167253.

References

Brown, A.K., Li, J., Pavot, C.M., Lu, Y., 2003. A lead-dependent DNAzyme with a two-step mechanism. Biochemistry 42, 7152–7161.

Chen, X., Wang, X., Lu, Z., Luo, H., Dong, L., Ji, Z., Xu, F., Hou, D., Hou, C., 2020. Ultrasensitive detection of Pb^{2+} based on DNAzymes coupling with multi-cycle strand displacement amplification (M-SDA) and nano-graphene oxide. Sensors Actuators B Chem. 311, 127898.

Deshmukh, M.A., Bodkhe, G.A., Shirsat, S., Ramanaviciene, A., Shirsat, M.D., 2018a. Nanocomposite platform based on EDTA modified Ppy/SWNTs for the sensing of Pb (II) ions by electrochemical method. Front. Chem. 26, 451.

Deshmukh, M.A., Celiesiute, R., Ramanaviciene, A., Shirsat, M.D., Ramanavicius, A., 2018b. EDTA_PANI/SWCNTs nanocomposite modified electrode for electrochemical determination of copper (II), lead (II) and mercury (II) ions. Electrochim. Acta 259, 930–938.

Deshmukh, M.A., Shirsat, M.D., Ramanaviciene, A., Ramanavicius, A., 2018c. Composites based on conducting polymers and carbon nanomaterials for heavy metal ion sensing (review). Crit. Rev. Anal. Chem. 48, 293–304.

El-Kady, M.M., Ansari, I., Arora, C., Rai, N., Soni, S., Verma, D.K., Singh, P., Mahmoud, A.E.D., 2023. Nanomaterials: a comprehensive review of applications, toxicity, impact, and fate to environment. J. Mol. Liq. 370, 121046.

Gao, H., Koopmans, G.F., Song, J., Groenenberg, J.E., Liu, X., Comans, R.N.J., Weng, L., 2022. Evaluation of heavy metal availability in soils near former zinc smelters by chemical extractions and geochemical modelling. Geoderma 423, 115970.

Geng, F., Wang, D., Feng, L., Li, G., Xu, M., 2020. An improved structure-switch aptamer-based fluorescent Pb^{2+} biosensor utilizing the binding induced quenching of AMT to G-quadruplex. Chem. Commun. 56, 10517–10520.

Guan, H., Yang, S., Zheng, C., Zhu, L., Sun, S., Guo, M., Hu, X., Huang, X., Wang, L., Shen, Z., 2021. DNAzyme-based sensing probe protected by DNA tetrahedron from nuclease degradation for the detection of lead ions. Chem. Commun. 57, ACS Sens.

Huang, Z., Chen, J., Luo, Z., Wang, X., Duan, Y., 2019. Label-free and enzyme-free colorimetric detection of Pb^{2+} based on RNA cleavage and annealing-accelerated hybridization chain reaction. Anal. Chem. 91, 4806–4813.

Ibrahim, E.A., El-Sherbini, M.A.A., Selim, E.M., 2022. Effects of biochar on soil properties, heavy metal availability and uptake, and growth of summer squash grown in metal-contaminated soil. Sci. Hortic. 301, 111097.

Ji, R., Niu, W., Chen, S., Xu, W., Ji, X., Yuan, L., Zhao, H., Geng, M., Qiu, J., Li, C., 2019. Target-inspired Pb^{2+}-dependent DNAzyme for ultrasensitive electrochemical sensor based on MoS$_2$-AuPt nanocomposites and hemin/Gquadruplex DNAzyme as signal amplifier. Biosens. Bioelectron. 144, 111560.

Lan, L., Yao, Y., Ping, J., Ying, Y., 2019. Ultrathin transition-metal dichalcogenide nanosheet-based colorimetric sensor for sensitive and label-free detection of DNA. Sensors Actuators B Chem. 290, 565–572.

Li, Y., Li, H., Fang, W., Liu, D., Liu, M., Zheng, L., Zhang, L., Yu, H., Tang, H., 2022. Amplification of the fluorescence signal with clustered regularly interspaced short palindromic repeats-Cas12a based on Au nanoparticle-DNAzyme probe and on-site detection of Pb^{2+} via the photonic crystal chip. ACS Sens. 7, 1572–1580.

Li, H., Xie, Y., Chen, F., Bai, H., Xiu, L., Zhou, X., Guo, X., Hu, Q., Yin, K., 2023. Amplification-free CRISPR/Cas detection technology: challenges, strategies, and perspectives. Chem. Soc. Rev. 52, 361–382.

Liang, W., Wang, X., Zhang, X., Niu, L., Wang, J., Wang, X., Zhao, X., 2023. Water quality criteria and ecological risk assessment of lead (Pb) in China considering the total hardness of surface water: a national-scale study. Sci. Total Environ. 858, 159554.

Lindsay, W.L., Norvell, W.A., 1978. Development of a DTPA soil test for zinc, iron, manganese, and copper. Soil Sci. Soc. Am. J. 42, 421–428.

Liu, J., Lu, Y., 2004. Accelerated color change of gold nanoparticles assembled by DNAzymes for simple and fast colorimetric Pb^{2+} detection. J. Am. Chem. Soc. 126, 12298–12305.

Liu, X., Yao, Y., Ying, Y., Ping, J., 2019. Recent advances in nanomaterial-enabled screen-printed electrochemical sensors for heavy metal detection. Trends Anal. Chem. 115, 187–202.

Lv, Y., Sun, Y., Liu, W., Yu, J., Jing, G., Liu, W., Xia, H., Li, D., Li, W., 2022. Enzyme-free dual-amplification assay for colorimetric detection of tetracycline based on Mg^{2+}-dependent DNAzyme assisted catalytic hairpin assembly. Talanta 241, 123214.

Malematja, E., Manyelo, T.G., Sebola, N.A., Kolobe, S.D., Mabelebele, M., 2023. The accumulation of heavy metals in feeder insects and their impact on animal production. Sci. Total Environ. 885, 163716.

Mao, M., Yan, T., Chen, G., Zhang, J., Shi, L., Zhang, D., 2021. Selective capacitive removal of Pb^{2+} from wastewater over redox-active electrodes. Environ. Sci. Technol. 55, 730–737.

McConnell, E.M., Cozma, I., Mou, Q., Brennan, J.D., Lu, Y., Li, Y., 2021. Biosensing with DNAzymes. Chem. Soc. Rev. 50, 8954–8994.

Meng, L., Liu, M., Xiao, K., Zhang, X., Du, C., Chen, J., 2020. Sensitive photoelectrochemical assay of Pb^{2+} based on DNAzyme-induced disassembly of the "Z-scheme" TiO$_2$/Au/CdS QDs system. Chem. Commun. 56, 8261–8264.

Miao, X., Ling, L., Shuai, X., 2011. Ultrasensitive detection of lead(II) with DNAzyme and gold nanoparticles probes by using a dynamic light scattering technique. Chem. Commun. 47, 4192–4194.

Parker, D.R., Pedler, J.F., 1997. Reevaluating the free-ion activity model of trace metal availability to higher plants. Plant Soil 196, 223–228.

Rajaji, P., Panneerselvam, P., 2020. A novel polydopamine grafted 3D MOF nanocubes mediated GR-5/GC DNAzyme complex with enhanced fluorescence emission response toward spontaneous detection of Pb(II) and Ag(I) ions. ACS Omega 5, 25188–25198.

Rensing, C., Maier, R.M., 2003. Issues underlying use of biosensors to measure metal bioavailability. Ecotoxicol. Environ. Saf. 56, 140–147.

Song, X., Wang, Y., Liu, S., Zhang, X., Wang, J., Wang, H., Zhang, F., Yu, J., Huang, J., 2019. A triply amplified electrochemical lead(II) sensor by using a DNAzyme and via formation of a DNA-gold nanoparticle network induced by a catalytic hairpin assembly. Microchim. Acta 186, 559.

Suo, Z., Qi, X., Dong, J., Wei, M., He, B., Jin, H., Guo, R., Ren, W., Xu, Y., 2023. An efficient electrochemical biosensor for the detection of heavy metal lead in food based on magnetic separation strategy and Y-DNA structure. Anal. Methods 15, 1306–1314.

Teng, W., Zhao, J., Li, Q., Shi, P., Zhang, J., Yan, M., Zhang, S., 2023. A DNAzyme-mediated signal amplification biosensor for ultrasensitive detection of lead ions based on SERS tags. Sens. Diagn. 2, 132–139.

Tessier, A., Campbell, P.G.C., Bisson, M., 1979. Sequential extraction procedure for the speciation of particulate trace metals. Anal. Chem. 51, 844–851.

Ure, A.M., Quevauviller, P., Muntau, H., Griepink, B., 1993. Speciation of heavy metals in soils and sediments. An account of the improvement and harmonization of extraction techniques undertaken under the auspices of the BCR of the Commission of the European Communities. Int. J. Environ. Anal. Chem. 51, 135–151.

Wang, H., Xie, Y., Wang, Y., Lai, G., 2022a. Target biorecognition-triggered assembly of a G-quadruplex DNAzyme-decorated nanotree for the convenient and ultrasensitive detection of antibiotic residues. Sci. Total Environ. 813, 152629.

Wang, Q., Wang, J., Huang, Y., Du, Y., Zhang, Y., Cui, Y., Kong, D., 2022b. Development of the DNA-based biosensors for high performance in detection of molecular biomarkers: more rapid, sensitive, and universal. Biosens. Bioelectron. 197, 113739.

Wen, Z., Liang, W., Zhuo, Y., Xiong, C., Zheng, Y., Yuan, R., Chai, Y., 2017. An efficient target-intermediate recycling amplification strategy for ultrasensitive fluorescence assay of intracellular lead ions. Chem. Commun. 53, 7525–7528.

Xu, C., Lan, L., Yao, Y., Ping, J., Li, Y., Ying, Y., 2018. An unmodified gold nanorods-based DNA colorimetric biosensor with enzyme-free hybridization chain reaction amplification. Sensors Actuators B Chem. 273, 642–648.

Xu, C., Ying, Y., Ping, J., 2019. Colorimetric aggregation assay for kanamycin using gold nanoparticles modified with hairpin DNA probes and hybridization chain reaction-assisted amplification. Microchim. Acta 186, 448.

Xu, C., He, M., Chen, B., Hu, B., 2022. Magnetic porous coordination networks for preconcentration of various metal ions from environmental water followed by inductively coupled plasma mass spectrometry detection. Talanta 245, 123470.

Yang, C., Yu, P., Li, Y., Wang, J., Ma, X., Liu, N., Lv, T., Zheng, H., Wu, H., Li, H., Sun, C., 2022a. Platform formed from ZIF-8 and DNAzyme: "turn-on" fluorescence assay for simple, high-sensitivity, and high-selectivity detection of Pb^{2+}. J. Agric. Food Chem. 70, 9567–9576.

Yang, H., Li, F., Xue, T., Hhan, M.R., Xia, X., Busquets, R., Gao, H., Dong, Y., Zhou, W., Deng, R., 2022b. Csm6-DNAzyme tandem assay for one-pot and sensitive analysis of lead pollution and bioaccumulation in mice. Anal. Chem. 94, 16953–16959.

Yang, H., Liu, Y., Wan, Y., Dong, Y., He, Q., Khan, M.R., Busquets, R., He, G., Zhang, J., Deng, R., Zhao, Z., 2023. DNAzyme-templated exponential isothermal amplification for sensitive detection of lead pollution and high-throughput screening of microbial biosorbents. Sci. Total Environ. 863, 160899.

Yao, Y., Wu, H., Ping, J., 2019. Simultaneous determination of Cd(II) and Pb(II) ions in honey and milk samples using a single-walled carbon nanohorns modified screen-printed electrochemical sensor. Food Chem. 274, 8–15.

Zhao, Y., Yavari, K., Wang, Y., Pi, K., Cappellen, P.V., Liu, J., 2022. Deployment of functional DNA-based biosensors for environmental water analysis. TrAC Trends Anal. Chem. 153, 116639.

Zheng, J., Wai, J.L., Lake, R.J., New, S.Y., He, Z., Lu, Y., 2021. DNAzyme sensor uses chemiluminescence resonance energy transfer for rapid, portable, and ratiometric detection of metal ions. Anal. Chem. 93, 10834–10840.